



Biotic and Abiotic Control Over Diurnal CH₄ Fluxes in a Temperate Transitional Poor Fen Ecosystem

Alexandre Lhosmot,^{1*} Adrien Jacotot,^{2,3} Marc Steinmann,¹ Philippe Binet,¹ Marie-Laure Toussaint,¹ Sébastien Gogo,⁴ Daniel Gilbert,¹ Sarah Coffinet,⁴ Fatima Laggoun-Deffarge,² and Guillaume Bertrand^{1,5}

¹Chrono-Environnement, UMR6249, CNRS, Université de Bourgogne Franche-Comté, Besançon, France; ²Institut Des Sciences de La Terre d'Orléans (ISTO), UMR7327, CNRS, Université d'Orléans, Orléans, France; ³Institut National de la Recherche en Agriculture, Alimentation et Environnement (INRAE), UMR 1069 SAS, 5 rue de Saint-Brieuc, 35042 Rennes, France; ⁴ECOBIO (Écosystèmes, Biodiversité, Évolution)-UMR 6553, Université de Rennes, CNRS, Renne, France; ⁵Water Resources and Environmental Engineering Laboratory, Federal University of Paraíba, Joao Pessoa 58051-900, Brazil

ABSTRACT

To understand the variability of methane (CH₄) fluxes between a temperate mid-altitude *Sphagnum*-dominated peatland and the atmosphere, we monitored simultaneously eddy covariance, hydrometeorological and physical parameters between April 2019 and December 2021. The site was a CH₄ source for the atmosphere, with a cumulative emission of $23.9 \pm 0.6 \text{ g C m}^{-2} \text{ year}^{-1}$. At the interannual scale, deeper water table during vegetation growth periods resulted in lower CH₄ fluxes (FCH₄), and reciprocally. Furthermore, the seasonal temperature variation in the anaerobic peat layer was a good predictor for FCH₄. However, while the lowest temperatures occurred between December and February, the lowest FCH₄ were observed between March and May, with around 30% of negative FCH₄. Indeed, the fastest increase

in temperature of the aerobic layer likely stimulated methanotrophy at the expense of methanogenesis. Negative FCH₄, systematically observed at midday, were concurrent with high photon flux densities, latent heat fluxes and net negative ecosystem CO₂ exchanges, suggesting the control of photosynthesis over CH₄ oxidation. Moreover, our results highlighted marked diurnal cycles with FCH₄ maximal at night and minimal at midday for all seasons. This diurnal cyclicity is in opposition to what is typically known for peatlands dominated by vascular plants. Physical parameters, such as soil surface temperature and sensible heat fluxes, likely contribute to this diurnal FCH₄ cyclicity and require further investigation. Our study thus demonstrates that diurnal variations in FCH₄ must be considered before upscaling to seasonal or annual cycles, along with the effect of vegetation on CH₄ transfer and oxidation processes.

Received 23 July 2022; accepted 21 November 2022;
published online 1 December 2022

Supplementary Information: The online version contains supplementary material available at <https://doi.org/10.1007/s10021-022-00809-x>.

Author Contributions: AL wrote the original draft. AL, AJ and GB participated to the conception of the study, designed methodology and analyzed data. AJ and MLT acquired eddy covariance and soil meteorological data. All authors contributed to the writing and approved the final version of the manuscript.

*Corresponding author; e-mail: alexandre.lhosmot@univ-fcomte.fr

Key words: peatland ecosystem; diurnal cycle; methane flux; methane oxidation; sphagnum; temperate ecosystem; eddy covariance.

HIGHLIGHTS

- FCH₄ were lower during daytime and higher at night throughout the year.
- Negative FCH₄ where concomitants with negative NEE.
- Diurnal FCH₄ amplitude followed a seasonal trend.

INTRODUCTION

Peatlands host one third of the Earth total soil organic carbon, although they cover only 3% of the continental surface (Gorham 1991; Xu and others 2018). These vegetated and waterlogged ecosystems can be considered as biogeochemical and carbon hot spots of the Critical Zone, which is defined as the thin layer of the Earth from the top of the canopy to the unaltered rocks that shelters life and the biogeochemical cycles (Anderson and others 2004; Gaillardet and others 2018). Permanent anaerobic and reduced redox conditions in peatlands limit organic matter degradation and its transformation to carbon dioxide (CO₂), resulting in peatlands being a carbon reservoir that had accumulated over centennial to millennial time scales.

Waterlogged conditions promote the microbial production of methane (CH₄) that is then emitted to the atmosphere and has a radiative power 28–34 times greater than CO₂ (Lai 2009; IPCC 2013; Stepniewska and Goraj 2014). The net CH₄ flux to the atmosphere is not only dependent on its production under anoxic conditions, but also on its transfer to the surface. This transfer occurs through molecular diffusion, ebullition or through aerenchymatous tissues (Sebacher and others 1985; Chanton and Dacey 1991; Windsor and others 1992). In parallel, a part of CH₄ may be consumed by methanotrophs in the presence of oxygen, especially in the aerobic surface layer, or in anaerobic conditions through oxidative pathways using different electron acceptor such as nitrate, sulfate or iron (III) (Lai 2009; Smemo and Yavitt 2011; Stepniewska and Goraj 2014; Shi and others 2017). In addition, CH₄ flux (FCH₄) balance results from the interactions of numerous physico-chemical factors such as Water Table Depth (WTD), vegetation cover and temperature (Turetsky and others 2014; Leroy and others 2017; Li and others 2021; Zhang and others 2021). Among these factors, temperature is a key predictor for seasonal CH₄ production in the anaerobic peat layer (Dun-

field and others 1993; Long and others 2009; van Winden and others 2012; Stepniewska and Goraj 2014; Knox and others 2021). In contrast, the lowering of the WTD favored by high temperature and evapotranspiration favors oxygenation of the peat column that, in turn, limits CH₄ emissions (Lai 2009; Stepniewska and Goraj 2014; Bertrand and others 2021). At the diurnal scale, FCH₄ can widely vary in both shape and amplitude within peatland types and seasons (Nadeau and others 2013; Dooling and others 2018; Knox and others 2021).

Saunois and others (2020) estimated that over the period 2000–2017 wetlands, at the global scale, including peatlands, contributed 25–30% of the worldwide CH₄ emissions. However, the specific contribution of peatlands to these CH₄ emissions remains uncertain because of the multitude and complexity of controlling parameters to set in the models (Saunois and others 2020; Salmon and others 2021). However, both climatic and land-use change modify hydrometeorological conditions of peatlands, which do not only impact their distribution, size and vegetation cover, but also potentially the balance between CH₄ production and oxidation. The heterogeneity of peatland types and sizes associated with complex interactions between hydrology, carbon cycle and vegetation dynamics make their response to climate change and anthropogenic disturbances difficult to predict (Loisel and others 2021; Riutta and others 2020).

In addition, although numerous studies focused on boreal peatlands, the temperate ones remain understudied, especially temperate montane peatlands (Rosset and others 2019). However, temperate peatlands might be considered “as ‘ecosystem sentinels’ for climate change, acting as early warning indicators of climate-carbon feedbacks” as it was proposed by Briones and others (2022). Beyond, peatland monitoring combining hydrometeorological variables and greenhouse gas (GHG) fluxes in a wide panel of altitude and latitude, vegetation cover and degree of anthropogenic impact participate to build a robust database. Such a database is essential to evaluate peatland restoration strategies that induce, through rewetting, an increase in FCH₄ (Abdalla and others 2016). Monitoring of GHG fluxes, covering from interannual to diurnal scale including dormant season, is enabled by the eddy covariance technique that has been developing over the last 25 years (Morin 2019). Diurnal cycle studies on peatland FCH₄ prove to be important as the majority of FCH₄ are measured only during daytime with the incubation chamber method (Denmead 2008; Dooling and others 2018). Therefore, the comprehension of this

diurnal cycle remains a challenge in order to improve annual CH₄ budget of a peatland when only daytime measurements are available (Dooling and others 2018).

In this context, this work aims to document current temperate peatland CH₄ dynamic by delineating the biotic and abiotic processes influencing FCH₄. Considering the range of possible constraints over FCH₄, deconvoluting these factors may be helped by long-term and high frequency monitoring. In this perspective, we jointly investigated WTD, soil and air temperatures, Photosynthetic Photon Flux Density (PPFD), latent and sensible heat fluxes (LE and H), Net Ecosystem CO₂ Exchange (NEE) and FCH₄ during 2.5 years. This allowed us to address multiannual, seasonal and diurnal CH₄ patterns of a temperate mid-altitude *Sphagnum*-dominated transitional poor fen, located in the Jura Mountains in Eastern France (Forbonnet peatland).

MATERIAL AND METHODS

Study site

The study was conducted at the Forbonnet peatland, located at a mid-latitude and mid-altitude position (N46.826, E6.1754, 840 m a.s.l.) in the French Jura Mountains within the Frasné–Bouverans peatland complex (~ 300 ha; Lhosmot and others 2021). The site is one of the four peatlands of the French National Peatland Observatory Service (SNO Tourbières; Gogo and others 2021), being also an observatory of the French research infrastructure of the Critical Zone (OZCAR; Gaillardet and others 2018).

This ecosystem is located in a karstic syncline made of Jurassic and Cretaceous marls and limestones, partially covered by glacial impermeable deposits favoring water accumulation and development of peatlands. The study site corresponds to a *Sphagnum*-dominated peatland (~ 7 ha) belonging to a larger peatland complex of around 300 ha that is recognized for its biodiversity (Natura 2000, Ramsar Convention, Regional Natural Reserve). This peatland is supplied in water by (1) local rainfall, (2) lateral flow from the surrounding by topographically higher more mature and wooded peatlands and (3) by localized and intermittent mineralized groundwater from moraines and/or karst system (Lhosmot and others 2021). The upper peat layer remains the most acidic and least mineralized one with pH varying from 4 to 5.5.

The climate is temperate with a marked continental influence, straddling between Cfb and Dfb

according to the Köppen–Geiger climate classification (Rubel and others 2017). More particularly, the site is subjected to contrasted seasons with mean monthly temperatures ranging from 0 °C (December to February) to 15 °C in July and August while the annual average is about 7 °C (2009–2020). Precipitation events are regularly distributed over the year with a mean of 135 ± 25 mm month⁻¹ (2009–2019).

Concerning the vegetation, the study area is mainly covered by *Sphagnum* spp mosses. *Andromeda polifolia*, *Vaccinium oxycoccos*, *Eriophorum vaginatum*, *Scheuchzeria palustris*, *Drosera* spp. and *Calluna vulgaris* are also present. *Pinus uncinata* occurs sparsely around the edges of the peatland. The micro-topography of the Forbonnet peatland edges features an alternance of hummocks and hollows supporting a mosaic of vegetation while the center of the system is relatively homogenous and flat and corresponds to a transitional poor fen (Delarue and others 2011; Buttler and others 2015).

GHG fluxes and Auxiliary Data Measurements

Methane (CH₄), carbon dioxide (CO₂), latent heat flux (LE) and sensible heat flux (H) were measured with an eddy covariance (EC) flux tower from the end of April 2019 to December 2021. Localization of the EC is available on the observatory website (Gogo and others 2021), and its footprint corresponds to the flat transitional poor fen dominated by *Sphagnum* (see Supplementary material 1). The EC footprint vegetation is dominated by *Sphagnum* spp (~ 80%), whereas vascular plants (mainly *Eriophorum vaginatum*) represent the rest of the vegetation (Bailly 2017). The EC system included an open-path CH₄ LI-7700 and an enclosed-path LI-7200/RS (LI-COR Biosciences, USA) to measure, respectively, CH₄ and both H₂O and CO₂ concentrations. Wind velocity and direction components as well as fast temperature readings were provided by a Gill HS-50 3D ultrasonic anemometer (Gill Instruments Limited, UK) placed at 2 m above the soil with a north offset of 220°. All data were sampled at a 20 Hz frequency and recorded through a LI-7550 Interface Unit (LI-COR Biosciences, USA).

Micro-meteorological measurements included PPFD (SKP115 Quantum Sensor, Skye Instruments Limited, UK), air temperature (T_{Air}) and relative humidity (RH; HMP155A, VAISALA, Finland). Soil measurements included Water Table Depth (WTD; CS451, Campbell Scientific) at one location and temperature (T_{Soil}) at 2, 5, 10, 25 and 60 cm

depths. T_{Soil} values at 2 and 5 cm are the mean of two replicated sensors. Intermediate depth temperatures (5, 10 and 25 cm) showed a gradual evolution between the 2 and 60 cm depths (see Supplementary material 2). Temperature was also recorded in a piezometer (T_{Peat}) integrating the complete catotelm profile (40–180 cm depth). All auxiliary data were recorded in a similar environment, beside the EC footprint (~ 75 m from the EC station). The data were measured every minute and then 30-min averaged.

Fluxes calculation

CH_4 , CO_2 , LE and H were calculated using EddyPro version 7.0.6 (LI-COR Biosciences, USA) and following the methods described by Vitale and others (2020) and references therein. Calculation included spikes count and removal (Mauder and others 2013), double-axis rotation for tilt correction (Wilczak and others 2001), covariance maximization for time-lag compensation, *in situ* spectral correction (Fratini and others 2012) and then 30-min block averaging. Cleaning of FCH4 was performed using the quality flags qualification of Mauder and Foken (2011), and accordingly, only fluxes with a flag 0 criterion were kept in the dataset. Cleaning of CO_2 fluxes was performed with the procedure of Vitale and others (2020) with the RFlux package in its non-ICOS version (Vitale and others 2021). In addition, due to the restricted area of the studied peatland and the location of the EC tower, only the fluxes recorded with a wind direction between 143 and 270°N were conserved during the cleaning procedure. The footprint surface estimation is based on aggregated half-hour measurements from April 2019 to December 2021 after wind direction filtration and following the method described by Kljun and others (2015) (Figure in Supplementary material 1).

Averaged FCH4 and CO_2 fluxes were corrected for periods of low friction velocity (u^*) that frequently appear at nighttime. The calculation of the threshold is based on the data and is thus specific and different for each dataset. The minimal u^* threshold for accepted fluxes was estimated by the method of Papale and others (2006) and implemented in the REddyProc algorithm developed by Wutzler and others (2018). Annual calculated thresholds were 0.043, 0.069 and 0.049 for 2019, 2020 and 2021. Following these results, we decided to take a unique threshold value of 0.075 for the three measurements years, which is upper than the calculated ones in order to ensure more robustness to the kept data. All fluxes below this threshold

were discarded from the dataset. Finally, the available CH_4 data covered 22% of the study period. The data gap in winter 2020–2021 is due to the removal of the analyzer because of excessive snow cover. In this study, a negative flux is defined as a flux from the atmosphere to the soil, and reciprocally.

The daily mean amplitude of FCH4 (maximum difference of fluxes between day and night) for each month was calculated as the difference between the mean FCH4 at night (PPFD $< 1 \mu\text{mol m}^{-2} \text{s}^{-1}$) and the minimum FCH4 of the day. Similarly, the daily mean amplitude of temperature in soil was calculated as the difference between the mean temperature at night (PPFD $< 1 \mu\text{mol m}^{-2} \text{s}^{-1}$) and the diurnal maximum temperature.

To estimate the annual FCH4 budget, FCH4 were gap-filled from 2019 to 2021 using the Random Forest (RF) method with T_{soil} , WTD, PPFD and u^* as input predictors. Although no standardized gap-filling method currently exists concerning CH_4 (Knox and others 2019), mostly due to its dependence to many environmental drivers, Kim and others (2020) recently showed a high performance of random forest algorithms (RF).

Statistical Analyses

Linear regressions and statistical analyses were realized using the SciPy library in python language (Jones and others 2001). Difference of annual and monthly means WTD was compared with the nonparametric Mann–Whitney U test as the main data were not normally distributed. All uncertainties given in the manuscript correspond to the standard deviation.

RESULTS

Environmental Variables

Monthly T_{Air} and T_{Soil} at 2 cm depth ($T_{\text{soil-2 cm}}$) showed similar variations with lowest values in January (~ 0 °C) and peaks in July for 2020 and June for 2021 (respectively, ~ 16 and ~ 18 °C, Figure 1A). For T_{Soil} at 60 cm depth ($T_{\text{soil-60 cm}}$), the seasonal peak was offset in August and the seasonal amplitude (~ 13 °C) was lower than for $T_{\text{soil-2 cm}}$ (~ 17 °C, Figure 1A). The mean monthly peat water temperature recorded in a piezometer (T_{Peat}) at 40 to 180 cm depth varied between 4.4 and 13.5 °C. For T_{Air} , the values ranged between -1 and 17 °C, for $T_{\text{soil-2 cm}}$ between 0.4 and 18.1 °C, and for $T_{\text{soil-60 cm}}$ between 2.9 and 15.6 °C. T_{Peat} reached its seasonal peak at the end of August (Figure 1A). PPFD

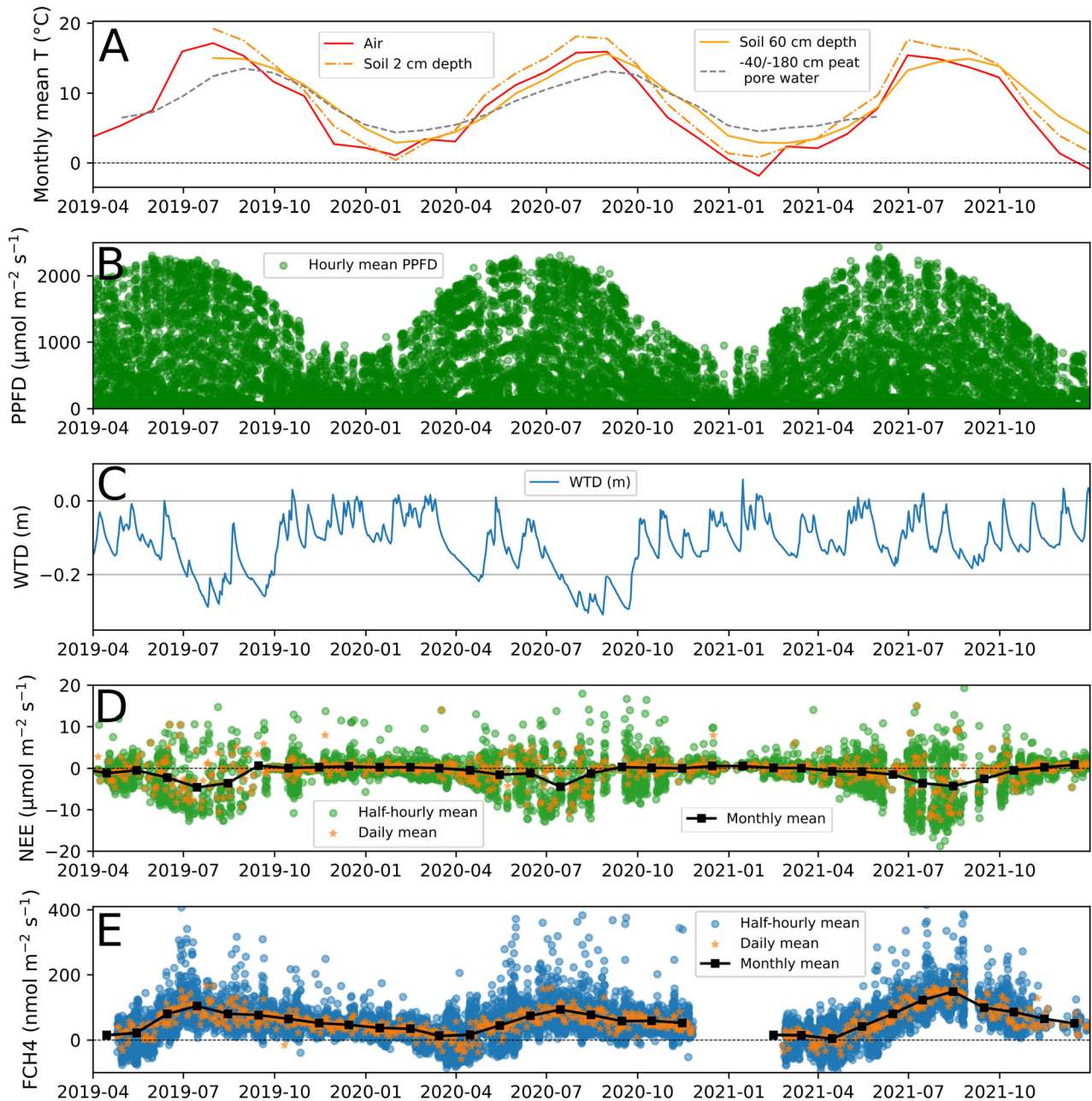


Figure 1. **A** Monthly mean temperature measured in different compartments of the ecosystem (°C). For T_{soil} only the 2 and 60 cm depths are plotted in Figure 1 to keep figures readable, for intermediate depths, see Supplementary data. **B** Hourly PPFD (μmol m⁻² s⁻¹). **C** Daily mean WTD (m). **D** Half-hourly, daily, and monthly NEE measured by eddy covariance (μmol m⁻² s⁻¹). The horizontal dashed line indicates the zero value. **E** Half hourly, daily, and monthly FCH₄ measured by eddy covariance (nmol m⁻² s⁻¹). The horizontal dashed line indicates the zero value, highlighting the negative FCH₄.

showed seasonal trends similar to T_{Air} with highest values in July (2300 μmol m⁻² s⁻¹) and lowest values in winter (< 800 μmol m⁻² s⁻¹; Figure 1B).

At the diurnal scale, PPFD, T_{Air} and T_{soil} were highest during the day. PPFD reached its maximum between 1 and 3 pm. T_{Air} and T_{soil}-2 cm reached

maximum values between 3 and 5 pm, whereas T_{soil}-60 cm was highest between 11 pm and 2 am. The amplitude of T_{soil} decreased with depth and remained, similar to T_{peat}, close to zero at 60 cm depth, reflecting the thermic inertia of peat (McKenzie and others 2007). The daily amplitude of T_{soil} at 2 and 5 cm depth was highest from April

to September and considerably lower for the rest of the year (at 2 cm from 3.2 to 10.1 °C, mean = 6.5 °C; at 5 cm from 1.9 to 5.5 °C, mean = 3.9 °C, Figure 2). For deeper levels (10, 25 and 60 cm), the daily mean amplitude did not exceed 2.2 °C (mean = 1 °C).

WTD remained at an average of -0.12 ± 0.07 m (Figure 1C, daily mean values). Seasonal variations featured greater depths from July to September in 2019, 2020 and 2021 (respectively, -0.21 ± 0.04 , -0.24 ± 0.04 and -0.10 ± 0.04) and shallower depths in winter (from -10 cm to occasional positive values). WTD in 2021 (-0.9 ± 0.05 m) was significantly higher than in 2019 (-0.11 ± 0.07 m, p -value < 0.05) and 2020 (-0.13 ± 0.08 m, p -value < 0.05). The monthly mean WTD compared year to year shows that for May, July, August and September the WTD was significantly higher in 2021 than in the two others years (p -value < 0.05).

Seasonal variability of NEE showed lower amplitude from November to March, where the majority of half-hour fluxes ranged from -4 to $+4$ $\mu\text{mol s}^{-1} \text{m}^{-2}$. Mean monthly NEE for this period ranged from 0 to $+1$ $\mu\text{mol s}^{-1} \text{m}^{-2}$. Higher NEE amplitude was measured in July–August months. Half-hour NEE ranged from approximately -13 to $+10$ $\mu\text{mol s}^{-1} \text{m}^{-2}$, and mean monthly NEE reached -5 $\mu\text{mol s}^{-1} \text{m}^{-2}$ (Figure 1D).

CH₄ Fluxes

Along the two and a half years covered by the EC measurements (April 2019 to December 2021),

measured mean daily FCH₄ were 57.5 ± 41 $\text{nmol m}^{-2} \text{s}^{-1}$. Annual budget from gap-filled data for 2019, 2020 and 2021 were, respectively, 23.4, 23.5 and 24.8 $\text{g C m}^{-2} \text{year}^{-1}$. Seasonal variation in FCH₄ was similar for the whole period of study (Figure 1E). Highest monthly average FCH₄ were recorded in July and August (respectively, from 92.5 to 122 with a mean of 106 $\text{nmol m}^{-2} \text{s}^{-1}$ and from 76.2 to 147.4 with a mean of 101.2 $\text{nmol m}^{-2} \text{s}^{-1}$), whereas lowest FCH₄ occurred in early spring (March and April monthly average, respectively, 13 to 14.8 and 4.8 to 16.1 $\text{nmol m}^{-2} \text{s}^{-1}$). Regarding the half-hour values, negative FCH₄ were most frequent between March and May, representing in average $30.8 \pm 8.5\%$ of the half hour measurements. In February, negative FCH₄ were more variable, comprised between 5.7% and 28.8% of measured FCH₄ in 2020 and 2021, respectively. In contrast, for all other months, negative FCH₄ only represented $1.1 \pm 1.5\%$ of measured FCH₄. In addition, the diurnal FCH₄ showed lowest values during daytime (11am–3 pm) for all month of the year (Figure 3). Amplitude of this cycle was the highest in spring and summer (103.9 ± 21 $\text{nmol m}^{-2} \text{s}^{-1}$) and the lowest from October to January (47.1 ± 20 $\text{nmol m}^{-2} \text{s}^{-1}$; Figure 2). Diurnal FCH₄ amplitude at the end of winter (February and March) was 75 ± 29 $\text{nmol m}^{-2} \text{s}^{-1}$.

Environmental Control on FCH₄

At the seasonal scale, monthly WTD showed complex relationships with monthly mean FCH₄ with a large variation in FCH₄ (from 15 to 140 nmol m^{-2}

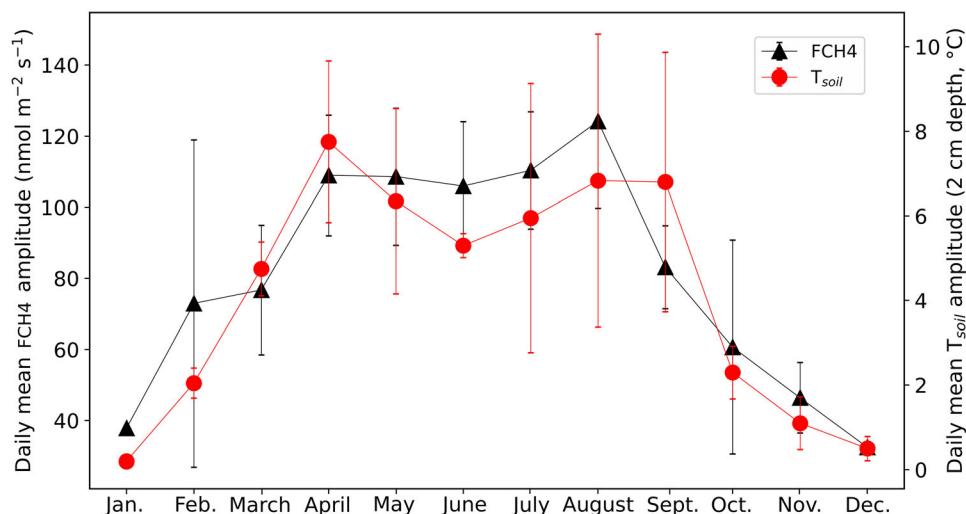


Figure 2. Monthly mean daily amplitude of FCH₄ ($\text{nmol m}^{-2} \text{s}^{-1}$) and soil temperature (°C, 2 cm depth). The vertical error bar corresponds to the standard deviation.

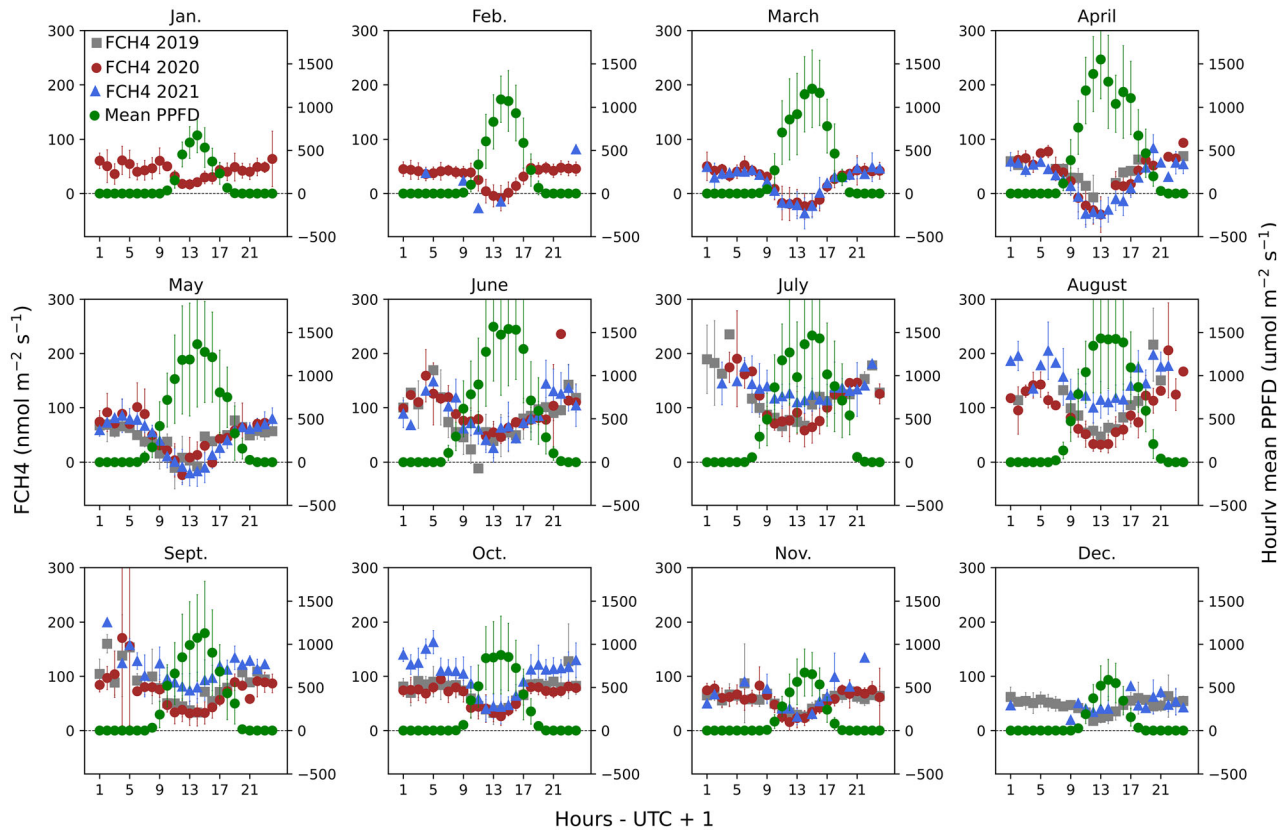


Figure 3. FCH₄ and PPFD for each month of the year (nmol and $\mu\text{mol m}^{-2} \text{s}^{-1}$). The vertical error bar represents the standard deviation. The data presented are hourly averages. The horizontal dashed line indicates the zero value.

2 s^{-1}) in a restricted WTD range of variation (-0.13 to -0.07 m), corresponding to 25% of the monthly WTD amplitude observed in our dataset (Figure 4).

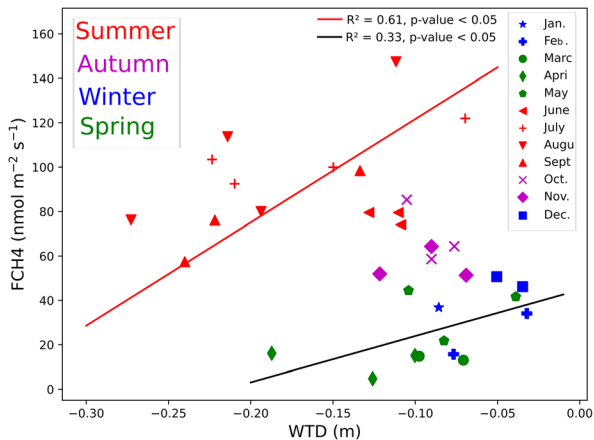


Figure 4. Scatter plot showing FCH₄ ($\text{nmol m}^{-2} \text{s}^{-1}$) function of WTD (monthly mean). The marker color indicates the season and the marker symbol the month of the year. The red linear regression ($R^2 = 0.61$) was calculated for months from July to September. The black linear regression ($R^2 = 0.33$) was calculated for months from January to May.

Nevertheless, a positive relationship between WTD and FCH₄ was detectable, but only for selected seasons. Positive relationships can be observed for the July–September and December–May periods where linear regressions were determined (Figure 4, respectively, R^2 equal to 0.61 and 0.33 and p -value < 0.05). In addition, the link between WTD and FCH₄ stood out by focusing on interannual cycles. For the July–September period, mean FCH₄ were higher in 2021, corresponding to the wettest summer (FCH₄ = $122.6 \pm 20 \text{ nmol m}^{-2} \text{s}^{-1}$ / WTD = $-0.10 \pm 0.05 \text{ m}$), than for the drier summers of 2019 and 2020 (FCH₄ = 86.5 ± 12 and $75.4 \pm 14 \text{ nmol m}^{-2} \text{s}^{-1}$, respectively; WTD = -0.21 ± 0.04 and $-0.24 \pm 0.04 \text{ m}$ with a drop at -0.31 m , respectively; Figure 1C and E).

To better understand the diurnal FCH₄ variations over the season, we decomposed the diurnal FCH₄ between the monthly mean FCH₄ at night (FCH₄-night) and the monthly mean of the daytime minimum (FCH₄-min-day). These two variables were plotted against the T_{soil-25 cm} that is considered as a proxy for seasonal CH₄ production variations (Figure 5, Ueyama and others 2020). Figure 5A shows that the FCH₄-night was posi-

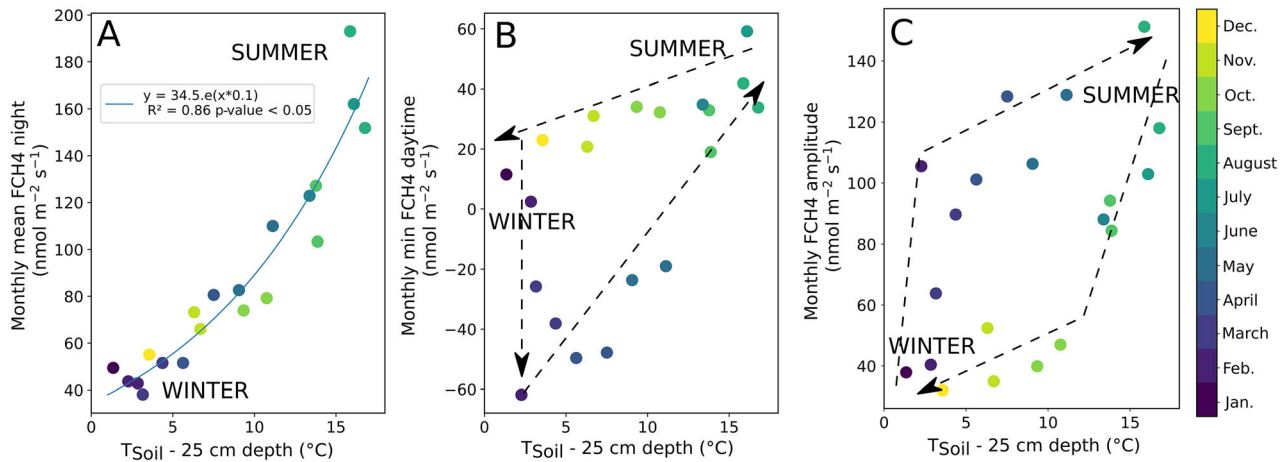


Figure 5. Scatter plots showing the relation between decomposed parts of the diurnal FCH₄ cycle and temperature at 25 cm depth (T_{Soil}-25 cm). T_{Soil}-25 cm was recorded from August 2019 to November 2021. Markers correspond to monthly averages. The color bar indicates the month of the year. The dashed arrows highlight the seasonal pattern of these variables and in particular the hysteresis. **A** The vertical axis is the average FCH₄ during the night (PPFD below 1 $\mu\text{mol m}^{-2} \text{s}^{-1}$ < /sup). **B** The vertical axis is the average minimum FCH₄ of the day. **C** The vertical axis is the average daily amplitude of FCH₄.

tively correlated with the T_{soil}-25 cm (exponential relation, $R^2 = 0.86$, p -value < 0.05). In contrast, the relation between the FCH₄-min-day and the T_{soil}-25 cm showed a complex pattern with a seasonal hysteresis, for example, lower values in spring (-20 to $-50 \text{ nmol m}^{-2} \text{ s}^{-1}$) than in autumn (20 to $30 \text{ nmol m}^{-2} \text{ s}^{-1}$, Figure 5B) for similar temperature (~ 5 – 10 °C). As a result of FCH₄-night and FCH₄-day-min dynamic, the monthly diurnal amplitude of FCH₄ also followed a hysteresis for similar T_{soil}-25 cm, for example, greater values during the end of winter and spring than during autumn and early winter (Figure 5C). This result indicates that temperature of saturated peat is not able to fully explain the seasonal variation in FCH₄-min-day.

Diurnal pattern of temperature (from air to soil 60 cm depth) was synchronous with FCH₄ despite a lag time from 2 to 12 h between the daily minimum FCH₄ (coming first) and the daily peak of T_{air} and T_{soil}-60 cm, respectively. Both the mean diurnal amplitude of FCH₄ and T_{soil}-2 cm followed the same seasonal trend (Figure 2).

Diurnal FCH₄ was also synchronous with PPFD, NEE, LE and H for all months of the year with daily peaks at mid-day (Figs. 3, 6, 7 and 8). FCH₄ was positively correlated with NEE and negatively correlated with PPFD, LE and H. Highest FCH₄ occurred at nighttime and concomitant with null PPFD and LE, negative H and positive NEE. The linear regressions between NEE and LE variables and FCH₄ were the most significant from March to

May with R^2 between 0.61 and 0.85 for NEE and 0.59 and 0.77 for LE (Figs. 6 and 7). For H and FCH₄ relationship, the linear regression was as strong in February ($R^2 = 0.89$) as in March to May (R^2 between 0.83 and 0.93, Figure 8).

DISCUSSION

FCH₄ Budget and Daily FCH₄ Dynamics

FCH₄ recorded in the Forbonnet between 2019 and 2021 indicated that the site acted as an annual net source of CH₄ to the atmosphere with an annual average budget of $23.9 \pm 0.6 \text{ g C m}^{-2}$, in the high range of those reported by Abdalla and others (2016) for northern peatlands (N40 to 70°; 95% CI of 7.6–15.7 g C m^{-2} and mean of $12 \pm 21 \text{ g C m}^{-2}$). Abdalla and others (2016) found that CH₄ emissions from fen ecosystems were significantly higher than those from bog, consistent with the significant emissions recorded at the Forbonnet. In addition, despite the site being located in a mountainous environment (840 m a.s.l.), the high CH₄ emissions were more consistent with its temperate location (N47°, mean annual T_{air} = 7 °C). For instance, Ueyama and others (2020) found, in a temperate bog (N43°, 16 m a.s.l) with comparable annual air temperature (mean = 7.2 ± 0.6 °C), annual CH₄ emissions between 13 and 19 g C m^{-2} . Beyond latitudinal and climatic influences, FCH₄ budget seems therefore highly site-dependent (Abdalla and others 2016).

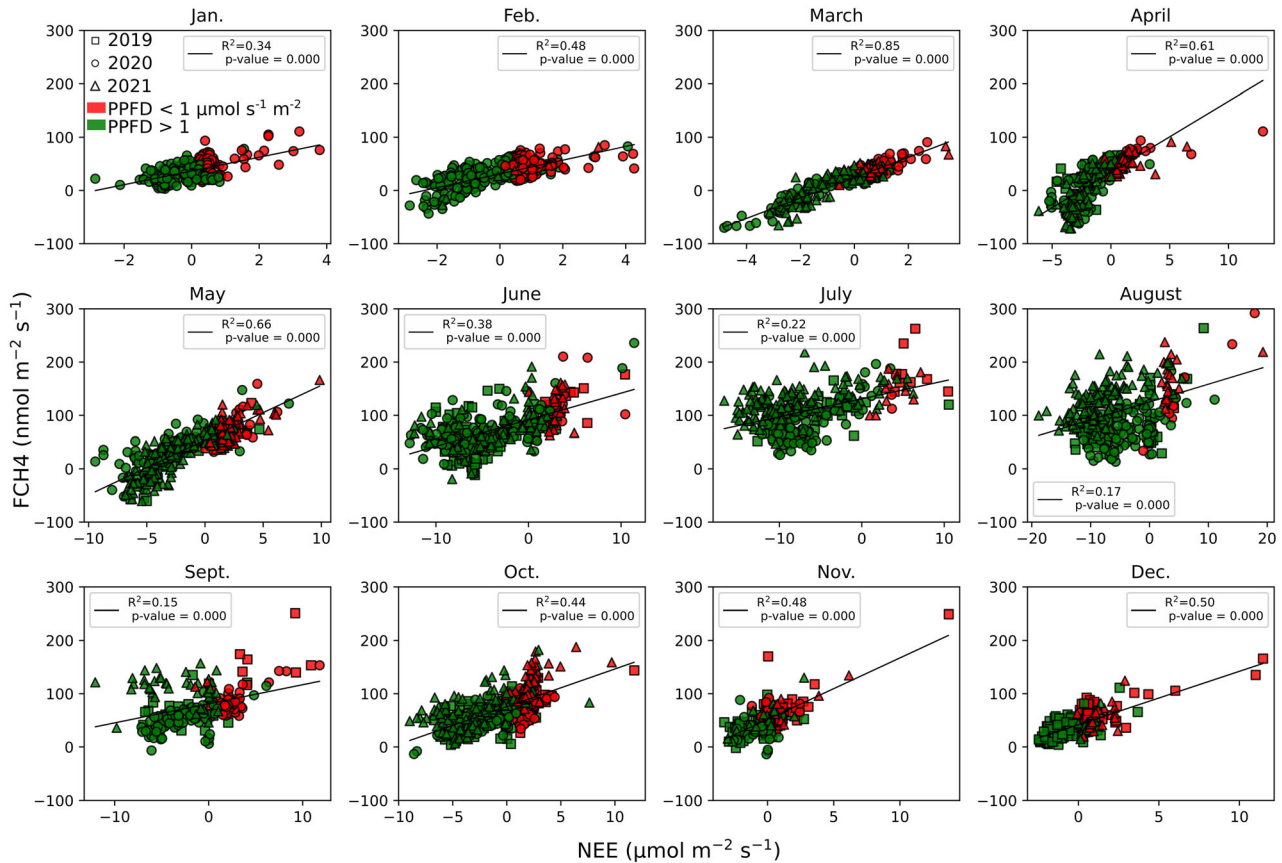


Figure 6. FCH₄ function of Net CO₂ Ecosystem Exchange (NEE) grouped by each month of the year (nmol and $\mu\text{mol m}^{-2} \text{s}^{-1}$, respectively). The data presented are half-hourly averages. The red color corresponds to conditions with PPFD below $1 \mu\text{mol m}^{-2} \text{s}^{-1}$. Reciprocally, the green color corresponds to conditions with PPFD higher than $1 \mu\text{mol m}^{-2} \text{s}^{-1}$. The black line is a linear regression including all points of the subplot.

Along the two and a half years of study, FCH₄ presented a diurnal cycle with higher values at night and lower values during the day, the minimum being reached around noon (Figure 3). This result is consistent with other temperate and boreal peatlands that showed similar shape of FCH₄ diurnal cycle (Yavitt and others 1990; Mikkilä and others 1995; Waddington and others 1996; Dooling and others 2018; Ueyama and others 2020). However, Nadeau and others (2013), in a boreal bog, or Greenup and others (2000) in a temperate bog, did not find such a clear daily variation. Beyond, Long and others (2009), focusing on summer periods in a boreal fen, measured no diurnal variations in June while the July month (peak of growing season) showed higher FCH₄ in daytime of about $20 \text{ nmol s}^{-1} \text{ m}^{-2}$. Consistent with this diurnal pattern, Knox and others (2021) observed distinct daytime/nighttime FCH₄ in 12 peatlands (four fen, four marshes, three rice paddies, one swamp and one bog) from the FLUXNET network dataset. These contrasted observations highlight the need to

better constraint the variables controlling the diurnal FCH₄ cycles in peatlands at various temporal scales. In particular, the shape of the diurnal cycle measured in this work highlights the need to distinct processes that may decrease FCH₄ during daytime to those that may contrariwise increase nighttime FCH₄. In this perspective, we discuss in the following the possible role of hydrological, thermal and photosynthetic processes on FCH₄.

WTD Influence on FCH₄

The respective thickness of the shallower aerobic and the deeper anaerobic peat layers is driven by the WTD variations (Sundh and others 1995; Turetsky and others 2008). In the present study, WTD remained at an average of -0.12 m , with occasional and relatively limited seasonal variations (minimum of -0.29 , -0.31 and -0.18 m depths in the summers of 2019, 2020 and 2021, respectively, Figure 1C). In parallel, at the interannual scale, FCH₄ is positively correlated with WTD. This

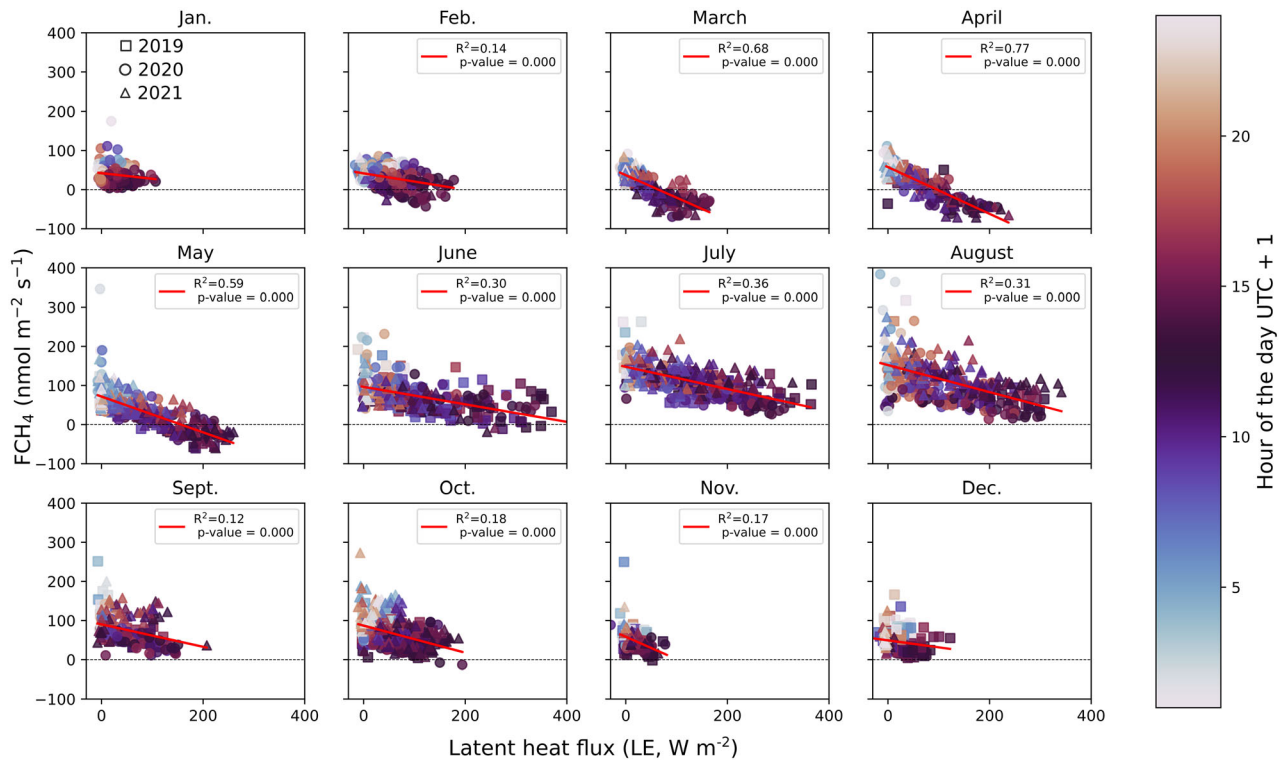


Figure 7. FCH₄ function of latent heat flux (LE) grouped by each month of the year (nmol m⁻² s⁻¹ and W m⁻², respectively). The data presented are half-hourly averages. The color code refers to the hour (UTC + 1) of the measurement. The red line is a linear regression including all points of the subplot. The horizontal dashed line indicates the zero value, highlighting the negative FCH₄.

is illustrated in summer (July to September) during which both WTD and FCH₄ were significantly higher in 2021 than in 2019 and 2020 (p -value < 0.05). Christensen and others (2003) and Knox and others (2021) suggested that CH₄ emission response to WTD variations mainly occurs for large WTD drops like those occurring during extreme events like drought. Consequently, as the WTD cannot fully explain the FCH₄ variability at seasonal scale, one must consider others seasonal processes such as thermal conditions and photosynthetic activity cycles.

Temperature Influence on Microbiological and Physical Controls on FCH₄

Seasonal variations in CH₄ emissions at the Forbonnet featured higher emissions in summer, and lower fluxes during the remaining part of the year, similar to emission variability observed in temperate-boreal peatlands exhibiting a distinct seasonal pattern of temperature (Lai 2009; Ueyama and others 2020; Knox and others 2021) (Figure 1A-E). However, the lowest and punctually even negative

FCH₄ occurred during spring while they were expected to occur during winter, when T_{soil} in the anaerobic peat layer is at its minimum, hence limiting biological activity (Figure 1A-E, Dunfield and others 1993; van Winden and others 2012).

As FCH₄ results from the balance between methanogenesis and methanotrophy, negative values are expected to occur when CH₄ oxidation surpasses its production. Hence, considering the acrotelm-catotelm model (Ingram 1978), relevant at the Forbonnet (Bertrand and others 2021; Lhosmot and others 2021), this suggests that the peat profile may, at the seasonal scale, be conceptualized as a two stacked biogeochemical reactor with reverse carbon dynamics due to contrasted redox conditions. First, the deep (catotelmic) anaerobic peat is expected to support CH₄ production in reduced conditions (Granberg and others 1997; Stepniewska and Goraj 2014). This is consistent with a CH₄ production highlighted at the Forbonnet by Lhosmot and others (2022) (under review) based on the observed $\delta^{13}\text{C}$ enrichment of the dissolved inorganic carbon in the catotelmic compartment. Second, the superficial, that is, acrotelmic, peat layer is expected to support CH₄

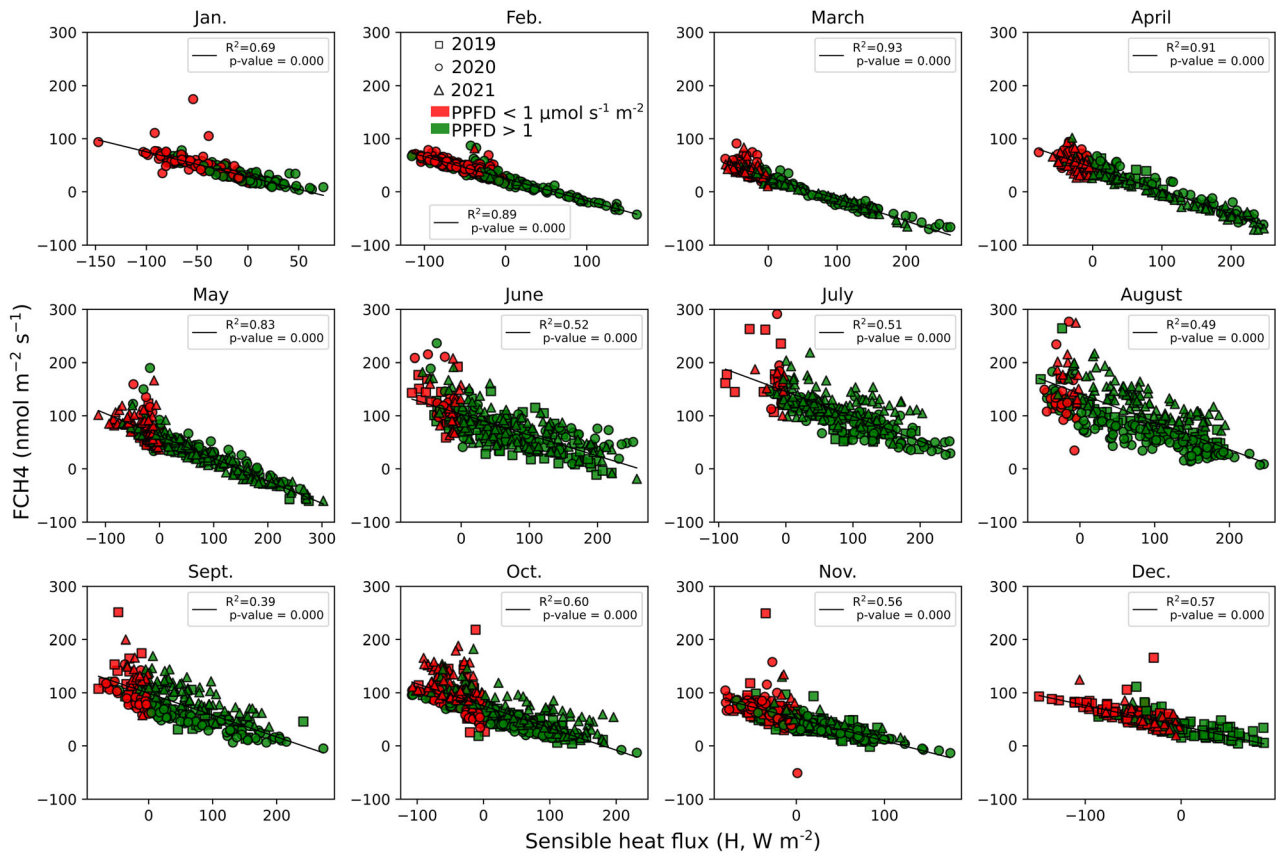


Figure 8. FCH₄ function of sensible heat flux (H) grouped by each month of the year ($\text{nmol m}^{-2} \text{s}^{-1}$ and W m^{-2} respectively). The data presented are half-hourly averages. The red color corresponds to conditions with PPFD below $1 \mu\text{mol m}^{-2} \text{s}^{-1}$. Reciprocally, the green color corresponds to conditions with PPFD higher than $1 \mu\text{mol m}^{-2} \text{s}^{-1}$. The black line is a linear regression including all points of the subplot.

oxidation due to a more variable waterlogging column favoring oxic conditions that shelter methanotrophs (Andersen and others 2013). This vertical delineation implies that the superficial methanotrophic peat reactor is stronger than the deep methanogenic reactor earlier in spring, due to progressive warming of the peat column from the surface (McKenzie and others 2007). Reversely, in autumn, the catotelm exhibits higher temperatures than the surface as the superficial peat progressively cools down and the deep peat CH₄ production is expected to exceed the superficial CH₄ oxidation (Figure 1A-E).

This two stacked biogeochemical reactor model agrees with the observed seasonal FCH₄ cycle (Figure 1E) and can be deepened by focusing on the dynamics of nocturnal and daily CH₄ separately (Figure 5 A, B, C). Hysteresis for FCH₄-day-min suggests that surface and aerobic control on FCH₄ occurred in addition to deep and anaerobic temperature (25 cm depth) seasonal variation. The impact of day-/nighttime surface temperature

variation on superficial processes is generally less clear than at the seasonal scale. Indeed, diurnal soil temperature and FCH₄ showed positive or negative correlations depending on the considered peatlands (Shannon and others 1996; Long and others 2009; Knox and others 2021). These contrasted observations suggest the combination of a range of processes at the diurnal scale that we propose to review under the light of the observed dynamics at the Forbonnet peatland.

First, the diurnal cycle of T_{soil} could play a role on methanotrophs as it is well established that temperature controls microbial activity (Andersen and others 2013). Lower temperature at night is expected to limit surface methanotrophy (Mikkilä and others 1995). However, the daily peak of surface T_{soil} occurred between three and five hours after the daily minimum FCH₄, suggesting that in addition to surface temperature other processes control daytime FCH₄ cycle. In contrast, as temperature at depth below 25 cm showed very limited diurnal variations (on average lower than $0.1 \text{ }^\circ\text{C}$),

this may favor a constant CH₄ production at the diurnal scale. Therefore, at the diurnal cycle, catotelmic thermal stability and superficial thermal variations likely favor constant methanogenesis and variable methanotrophy.

Second, we observed a negative and significant linear regression between FCH₄ and H (Figure 8), the highest H values occurring during nighttime. Koebisch and others (2015) and Godwin and others (2013) reported that as far as the radiation heat maintains the water thermal stratification, this would favor CH₄ trapping below the surface. In contrast, at night, water releases sensible heat leading to convective mixing and associated CH₄ emissions. Therefore, the diurnal variation in the vertical thermal gradient can increase nighttime FCH₄ due to changing physical conditions controlling CH₄ transfer.

A Photosynthesis Control over FCH₄?

The diurnal FCH₄ variability also showed a positive relationship with NEE. Notably, we observed an outstanding co-occurrence of negative NEE and FCH₄ at daytime (Figure 6). This suggests that plant activity may significantly influence CH₄ balance. Plant influence was previously reported (Greenup and others 2000; Dooling and others 2018; Knox and others 2021). Nevertheless, a great range of peatland FCH₄ evaluation such as those reported by Long and others (2009), Knox and others (2021) or Rey-Sanchez and others (2019) rather highlights greater FCH₄ at daytime and interpreted this pattern as the effect of vascular plant aerenchymatous tissues favoring CH₄ transfer to the atmosphere. They also found that LE, a proxy of plant activity and of CH₄ transport through plant tissues (Knox and others 2021), is positively correlated with FCH₄.

Even though such a process is not detectable in our study as FCH₄ was lower during the day and negatively correlated with LE (Figure 7), it is not excluded that the presence of vascular plants participates to FCH₄ diurnal cycle. Vascular plant photosynthesis produces labile organic matter, for example, acetate, that is transferred through the root system and used as substrate for methanogenesis (Rovira 1969; Whiting and others 1991; Ström and others 2003; Leroy and others 2017; Waldo and others 2019; Mitra and others 2020). Various studies showed that these root exudates are transformed into CH₄ within 24 h (Ström and others 2003; Mitra and others 2020; Knox and others 2021). This is consistent with the diurnal FCH₄ observed in our study. However, this time lag

may be variable and dependent of plant species (Ström and others 2003). Although Knox and others (2021) showed a lag time from one to four hours between the peak of green primary production (GPP) and the peak of CH₄ emissions, King and Reeburgh (2002) and Ström and others (2003) showed that CH₄ emitted from root exudates began after two hours and may reach a peak between three and seven days.

In contrast with a possible positive role of photosynthesis on nighttime FCH₄, but presumably limited because of the low abundance of vascular plant, plant photosynthetic activity may limit daytime FCH₄ as oxygen (O₂) penetration depth within the peat column increases during daytime (King 1990; Nedwell and Watson 1995; Frenzel and Karofeld 2000). This photosynthetic O₂ may then be used by methanotrophs to oxidize CH₄. In peatlands where vascular plants are not dominant such as at the Forbonnet, various organisms are known to be purveyors of O₂ by photosynthesis, essentially mosses, phototrophs (for example, microalgae, cyanobacteria) and mixotrophic protists (for example, ciliates) (Hamard and others 2021). Therefore, extrinsic microbial photosynthetic activity could be an important source of O₂ in the superficial peat pore water and contribute to limit daytime FCH₄. This hypothesis is reinforced by Song and others (2016) who showed at the Forbonnet that the first centimeters of *Sphagnum* were mainly covered by mixotrophs, and that phototrophs accounted for 19% of the microbial biomass. More generally, Hamard and others (2021) estimated that approximately 10% of the peatland's net primary O₂ production is due to this extrinsic superficial microbial photosynthesis. In addition, CH₄ may be directly oxidized within *Sphagnum* hyaline cells, where endosymbiotic methanotrophs were found to be active in both submerged and aerated conditions, providing up to 20% of the carbon used by the host plant (Kostka and others 2016; Raghoebarsing and others 2005). Consistently, Parmentier and others (2011) found in a Siberian peatland that this intrinsic symbiosis may result in a decline of 50% of CH₄ emissions in a *Sphagnum*-dominated area compared to an area without *Sphagnum* based on chamber measurements operated during one summer. Similar results were recently found in mesocosm experiments showing the positive effect of photosynthesis on CH₄ oxidation by *Sphagnum* (Kox and others 2020). As a result, at the Forbonnet, it is therefore hypothesized that the photosynthesis has a twofold impact on FCH₄. Firstly, a limiting constraint on FCH₄ associated with *Sphagnum* and mixotroph

photosynthesis coupled to CH₄ oxidation and, secondly, a nighttime FCH₄ increase associated with root exudates production of substrates for methanogenesis.

At the seasonal scale, the relationship between FCH₄ and both NEE and LE was the strongest at the end of winter and spring (March to May, Figures 6 and 7), suggesting a stronger photosynthetic control at that period. Accordingly, Campbell and Rydin (2019) and Moore and others (2006) showed that *Sphagnum* mosses stay photosynthetically active in winter and that the increase in photosynthesis at spring is initiated by bryophytes, respectively. In the same perspective, Korrensalo and others (2017) reported that *Sphagnum* photosynthesis was the highest during spring in an ombrotrophic peatland located in southern Finland. In addition, from March to May the period is generally wetter than the following summer (Figure 1C). The photosynthesis-derived O₂ might then be the overriding factor controlling O₂ availability and therefore CH₄ oxidation. Consistent with a greater spring activity, summer and autumn months featured a weaker relationship between FCH₄ and both NEE and LE. During summer, hot, dry and high PPFD conditions can induce photoinhibition of plants and in particular of *Sphagnum* whose primary production responds negatively to a decrease in the volumetric water content and increase in soil temperature (Murray and others 1993; Bragazza 2008; Norby and others 2019). Considering these elements, it is expected that *Sphagnum* photosynthesis and associated role on CH₄ dynamic become more impacted by the increase in droughts and

heatwaves frequency and intensity related to climate change (IPCC 2022).

Toward a Conceptual Model of FCH₄ Dynamic

The discussion proposed in the previous sections allows delineating an updated conceptual model synthesizing the biotic and abiotic controls on FCH₄ in *Sphagnum*-dominated peatlands (Figure 9). First, it is shown in “WTD Influence on FCH₄” section that interannual variation in WTD is negatively correlated with FCH₄ and controls the sizes of the aerobic and anaerobic peat layers. Second, at the seasonal scale (Temperature Influence on Microbiological and Physical Controls on FCH₄ section), the mean nocturnal FCH₄ variability is tightly linked to the anaerobic soil temperature (25 cm depth), suggesting a seasonal control over CH₄ production (Figure 5A). However, due to the thermic inertia of peat, the fastest increase in peat temperature in the aerobic layer at the end of the winter stimulates methanotrophic activity at the expense of methanogenic activity. This allows to explain the high density of negative FCH₄ from March to May. Then, in addition to the above-mentioned abiotic controls, the links of photosynthesis indicators (PPFD, LE, NEE) with diurnal and seasonal FCH₄, and especially its limitation (A Photosynthesis Control Over FCH₄ section), suggest that, photosynthesis associated with *Sphagnum* and microbiological activity might be conceptualized as a third compartment partially driving FCH₄ through its own dynamic.

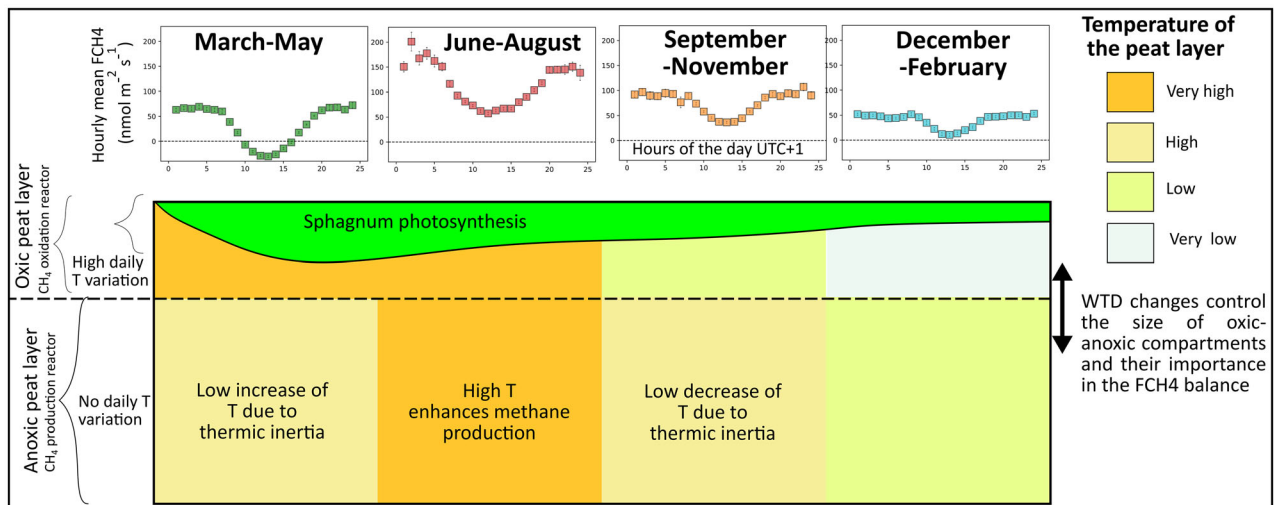


Figure 9. Conceptual model showing CH₄ dynamic according to biotic and abiotic seasonal and diurnal variations.

CONCLUSIONS AND PERSPECTIVES

This work investigated temporal variabilities of FCH₄ between a temperate and mid-altitude transitional mire and the atmosphere through eddy covariance measurements during two and half consecutive years. The site was an annual source of CH₄ whose emissions were controlled by a range of parameters, respectively, acting predominantly at contrasted time scales. In particular, our work highlights an outstanding role of photosynthesis activating daytime methanotrophy that clearly contrasts with sites where aerenchymatous plants dominated and where greater daytime FCH₄ are common.

In addition, the majority of diurnal FCH₄ found in literature were measured only in summer months or during the growing season. Here we measured the diurnal FCH₄ including the dormant stage of vegetation and evidenced complex seasonal variations. Thus, the proposed conceptual model is (Figure 9), to our knowledge, the first one to introduce a multi-temporal frame for the FCH₄ dynamics at the ecosystem scale in a temperate *Sphagnum*-dominated transitional poor fen.

In this framework and in order to better understand the CH₄ balance variability of peatlands, this model especially highlights the further need to (1) study both daytime and nighttime FCH₄ to improve CH₄ annual budget estimations and CH₄ peatland modeling at global scale (as suggested by Dooling and others 2018) and (2) to investigate and quantify the possible concurrent controls of microbiological and thermal stability over CH₄ emissions. In addition to the abiotic and biotic controls delineated in this study, such investigations could provide further drivers to constrain the future trajectories of *Sphagnum*-dominated peatlands under increasing climate changes.

ACKNOWLEDGEMENTS

The authors warmly thank the managers of the Regional Natural Reserve of Frasne-Bouverans for allowing access to the site, in particular Geneviève Magnon. This study is part of the CRITICAL PEAT project funded by the Bourgogne Franche-Comté Region (Accueil de Nouvelle Equipe de Recherche Agreement n°2019-Y09069), the SNO Tourbières (<https://www.sno-tourbieres.cnrs.fr/>) and the French Network of Critical Zone Observatories (OZCAR) Network (<https://www.ozcar-ri.org/fr/ozcar-observatoires-de-la-zone-critique-applicationset-recherche/>) as well as the THERMOPEAT project funded by OSU THETA. The SNO Tourbières

observing system was set up thanks to an incentive funding of the French Ministry of Research that allowed pooling together various pre-existing small-scale observation set-ups. The continuity of the field monitoring was made possible by continuous CNRS-INSU funding since 2008. A. Lhosmot benefits from a Ph.D. fellowship of the French Ministry of Research. Finally, the authors warmly thank the subject-matter editor as well as the two anonymous reviewers that provided detailed remarks and suggestions allowing a significant improvement in the manuscript.

DATA AVAILABILITY

Soil-meteorological and piezometers data are available on Zenodo repository (<https://doi.org/10.5281/ZENODO.3763342>; <https://doi.org/10.5281/ZENODO.3763766>) and also on the French National Peatland Observatory Service (SNO Tourbières, <https://www.sno-tourbieres.cnrs.fr/>). Detailed data are available upon request.

Declarations

Conflict of interest The authors declare that they have no conflict of interest.

REFERENCES

- Abdalla M, Hastings A, Truu J, Espenberg M, Mander Ü, Smith P. 2016. Emissions of methane from northern peatlands: a review of management impacts and implications for future management options. *Ecol Evol* 6:7080–7102.
- Andersen R, Chapman SJ, Artz RRE. 2013. Microbial communities in natural and disturbed peatlands: A review. *Soil Biology and Biochemistry* 57:979–994.
- Anderson SP, Blum J, Brantley SL, Chadwick O, Chorover J, Derry LA, Drever JI, Hering JG, Kirchner JW, Kump LR, Richter D, White AE. 2004. Proposed initiative would study Earth's weathering engine. *Eos Trans AGU* 85:265.
- Bailly G. 2017. Suivi floristique de la tourbière vivante de Frasne. Troisième passage, année 2017. Conservatoire botanique national de Franche-Comté – Observatoire régional des Invertébrés
- Bertrand G, Ponçot A, Pohl B, Lhosmot A, Steinmann M, Johannet A, Pinel S, Caldirak H, Artigue G, Binet P, Bertrand C, Collin L, Magnon G, Gilbert D, Laggoun-Deffarge F, Toussein M-L. 2021. Statistical hydrology for evaluating peatland water table sensitivity to simple environmental variables and climate changes application to the mid-latitude/altitude Frasne peatland (Jura Mountains, France). *Science of the Total Environment* 754:141931.
- Bragazza L. 2008. A climatic threshold triggers the die-off of peat mosses during an extreme heat wave. *Global Change Biology* 14:2688–2695.
- Briones MJJ, Juan-Ovejero R, McNamara NP, Ostle NJ. 2022. Microbial “hotspots” of organic matter decomposition in

- temperate peatlands are driven by local spatial heterogeneity in abiotic conditions and not by vegetation structure. *Soil Biology and Biochemistry* 165:108501.
- Buttler A, Robroek BJM, Laggoun-Défarge F, Jassey VEJ, Pochelon C, Bernard G, Delarue F, Gogo S, Mariotte P, Mitchell EAD, Bragazza L. 2015. Experimental warming interacts with soil moisture to discriminate plant responses in an ombrotrophic peatland. Morgan J, editor. *J Veg Sci* 26:964–974.
- Campbell C, Rydin H. 2019. The effects of winter stress on Sphagnum species with contrasting macro- and microdistributions. *Journal of Bryology* 41:205–217.
- Chanton JP, Dacey JWH. 1991. Effects of Vegetation on Methane Flux, Reservoirs, and Carbon Isotopic Composition. In: *Trace Gas Emissions by Plants*. Elsevier. pp 65–92. <https://linkinghub.elsevier.com/retrieve/pii/B978012639010050008X>. Last accessed 05/06/2022
- Christensen TR, Ekberg A, Ström L, Mastepanov M, Panikov N, Öquist M, Svensson BH, Nykänen H, Martikainen PJ, Oskarsson H. 2003. Factors controlling large scale variations in methane emissions from wetlands. *Geophys Res Lett* 30. <http://doi.wiley.com/https://doi.org/10.1029/2002GL016848>. Last accessed 15/01/2022
- Delarue F, Laggoun-Défarge F, Buttler A, Gogo S, Jassey VEJ, Disnar J-R. 2011. Effects of short-term ecosystem experimental warming on water-extractable organic matter in an ombrotrophic Sphagnum peatland (Le Forbonnet, France). *Organic Geochemistry* 42:1016–1024.
- Denmead OT. 2008. Approaches to measuring fluxes of methane and nitrous oxide between landscapes and the atmosphere. *Plant Soil* 309:5–24.
- Dooling GP, Chapman PJ, Baird AJ, Shepherd MJ, Kohler T. 2018. Daytime-only measurements underestimate CH₄ emissions from a restored bog. *Écoscience* 25:259–270.
- Dunfield P, Knowles R, Dumont R, Moore T. 1993. Methane production and consumption in temperate and subarctic peat soils: Response to temperature and pH. *Soil Biology and Biochemistry* 25:321–326.
- Fratini G, Ibrom A, Arriga N, Burba G, Papale D. 2012. Relative humidity effects on water vapour fluxes measured with closed-path eddy-covariance systems with short sampling lines. *Agricultural and Forest Meteorology* 165:53–63.
- Frenzel P, Karofeld E. 2000. CH₄ Emission from a Hollow-Ridge Complex in a Raised Bog: The Role of CH₄ Production and Oxidation. *Biogeochemistry* 51:91–112.
- Gaillardet J, Braud I, Hankard F, Anquetin S, Bour O, Dorfliger N, de Dreuzy JR, Galle S, Galy C, Gogo S, Gourcy L, Habets F, Laggoun F, Longuevergne L, Le Borgne T, Naaim-Bouvet F, Nord G, Simonneaux V, Six D, Tallec T, Valentin C, Abril G, Allemand P, Arènes A, Arfib B, Arnaud L, Arnaud N, Arnaud P, Audry S, Comte VB, Batiot C, Battais A, Bellot H, Bernard E, Bertrand C, Bessièrre H, Binet S, Bodin J, Bodin X, Boithias L, Bouchez J, Boudevillain B, Moussa IB, Branger F, Braun JJ, Brunet P, Caceres B, Calmels D, Cappelaere B, Celle-Jeanton H, Chabaux F, Chalikhakis K, Champollion C, Copard Y, Cotel C, Davy P, Deline P, Delrieu G, Demarty J, Dessert C, Dumont M, Emblanch C, Ezzahar J, Estèves M, Favier V, Faucheux M, Filizola N, Flammarion P, Flourey P, Fovet O, Fournier M, Francez AJ, Gandois L, Gascuel C, Gayer E, Genthon C, Gérard MF, Gilbert D, Gouttevin I, Grippa M, Gruau G, Jardani A, Jeanneau L, Join JL, Jourde H, Karbou F, Labat D, Lagadeuc Y, Lajeunesse E, Lastennet R, Lavado W, Lawin E, Lebel T, Le Bouteiller C, Legout C, Lejeune Y, Le Meur E, Le Moigne N, et al. 2018. OZCAR: The French Network of Critical Zone Observatories. *Vadose Zone Journal* 17:0.
- Godwin CM, McNamara PJ, Markfort CD. 2013. Evening methane emission pulses from a boreal wetland correspond to convective mixing in hollows. *J Geophys Res Biogeosci* 118:994–1005.
- Gogo S, Paroissien J, Laggoun-Défarge F, Antoine J, Bernard-Jannin L, Bertrand G, Binet P, Binet S, Bouger G, Brossard Y, Camboulive T, Caudal J, Chevrier S, Chiapiuso G, D'Angelo B, Durantez P, Flechard C, Francez A, Galop D, Gandois L, Gilbert D, Guimbaud C, Hinault L, Jacotot A, Le Moing F, Lerigoleur E, Le Roux G, Leroy F, Lhosmot A, Li Q, Machado da Silva E, Moquet J, Mora-Gomez J, Perdereau L, Rosset T, Toussaint M. 2021. The information system of the French Peatland Observation Service: Service National d'Observation Tourbières – a valuable tool to assess the impact of global changes on the hydrology and biogeochemistry of temperate peatlands through long term monitoring. *Hydrological Processes*:hyp. 14244.
- Gorham E. 1991. Northern Peatlands: Role in the Carbon Cycle and Probable Responses to Climatic Warming. *Ecological Applications* 1:182–195.
- Granberg G, Mikkilä C, Sundh I, Svensson BH, Nilsson M. 1997. Sources of spatial variation in methane emission from mires in northern Sweden: A mechanistic approach in statistical modeling. *Global Biogeochem Cycles* 11:135–150.
- Greenup AL, Bradford MA, McNamara NP, Ineson P, Lee JA. 2000. The role of Eriophorum vaginatum in CH₄ flux from an ombrotrophic peatland. *Plant and Soil*. 265–72.
- Hamard S, Céréghino R, Barret M, Sytiuk A, Lara E, Dorrepaal E, Kardol P, Küttim M, Lamentowicz M, Leflaive J, Le Roux G, Tuittila E, Jassey VEJ. 2021. Contribution of microbial photosynthesis to peatland carbon uptake along a latitudinal gradient. *J Ecol* 109:3424–3441.
- Ingram HAP. 1978. SOIL LAYERS IN MIRES: FUNCTION AND TERMINOLOGY. *J Soil Sci* 29:224–227.
- IPCC. 2013. *Climate Change 2013: The Physical Science Basis. Contribution of Working Group I to the Fifth Assessment Report of the Intergovernmental Panel on Climate Change*. Cambridge, United Kingdom and New York, NY, USA: Cambridge University Press
- IPCC. 2022. *Climate Change 2022: Impacts, Adaptation, and Vulnerability. Contribution of Working Group II to the Sixth Assessment Report of the Intergovernmental Panel on Climate Change*. [H-O Pörtner, DC Roberts, M Tignor, ES Poloczanska, K Mintenbeck, A Alegría, M Craig, S Langsdorf, S Löschke, V Möller, A Okem, B Rama (eds)].
- Jacotot A, Bertrand, Guillaume, Toussaint, Marie-Laure, Lhosmot, Alexandre, Gilbert, Daniel, Binet, Philippe, Gogo, Sébastien, Laggoun-Défarge, Fatima. 2022. Carbon and energy Eddy-covariance fluxes dataset collected at Frasne peatland (192ha, Jura Mountains, France). <https://zenodo.org/record/6025782>. Last accessed 10/02/2022
- Jones E, Oliphant T, Peterson P, and others. 2001. SciPy: Open Source Scientific Tools for Python. <http://www.scipy.org>
- Kim Y, Johnson MS, Knox SH, Black TA, Dalmagro HJ, Kang M, Kim J, Baldocchi D. 2020. Gap-filling approaches for eddy covariance methane fluxes: A comparison of three machine learning algorithms and a traditional method with principal component analysis. *Global Change Biology* 26:1499–1518.
- King GM. 1990. Regulation by light of methane emissions from a wetland. *Nature* 345:513–515.

- King J, Reeburgh WS. 2002. A pulse-labeling experiment to determine the contribution of recent plant photosynthates to net methane emission in arctic wet sedge tundra. *Soil Biology and Biochemistry* 34:173–180.
- Kljun N, Calanca P, Rotach MW, Schmid HP. 2015. A simple two-dimensional parameterisation for Flux Footprint Prediction (FFP). *Geoscientific Model Development* 8:3695–3713.
- Knox SH, Jackson RB, Poulter B, McNicol G, Fluet-Chouinard E, Zhang Z, Hugelius G, Bousquet P, Canadell JG, Saunio M, Papale D, Chu H, Keenan TF, Baldocchi D, Torn MS, Mammarella I, Trotta C, Aurela M, Bohrer G, Campbell DI, Cescatti A, Chamberlain S, Chen J, Chen W, Dengel S, Desai AR, Euskirchen E, Friberg T, Gasbarra D, Goded I, Goeckede M, Heimann M, Helbig M, Hirano T, Hollinger DY, Iwata H, Kang M, Klatt J, Krauss KW, Kutzbach L, Lohila A, Mitra B, Morin TH, Nilsson MB, Niu S, Noormets A, Oechel WC, Peichl M, Peltola O, Reba ML, Richardson AD, Runkle BRK, Ryu Y, Sachs T, Schäfer KVR, Schmid HP, Shurpali N, Sonnentag O, Tang ACI, Ueyama M, Vargas R, Vesala T, Ward EJ, Windham-Myers L, Wohlfahrt G, Zona D. 2019. FLUXNET-CH4 Synthesis Activity: Objectives, Observations, and Future Directions. *Bull Amer Meteor Soc* 100:2607–2632.
- Knox SH, Bansal S, McNicol G, Schafer K, Sturtevant C, Ueyama M, Valach AC, Baldocchi D, Delwiche K, Desai AR, Euskirchen E, Liu J, Lohila A, Malhotra A, Melling L, Riley W, Runkle BRK, Turner J, Vargas R, Zhu Q, Alto T, Fluet-Chouinard E, Goeckede M, Melton JR, Sonnentag O, Vesala T, Ward E, Zhang Z, Feron S, Ouyang Z, Alekseychik P, Aurela M, Bohrer G, Campbell DI, Chen J, Chu H, Dalmagro HJ, Goodrich JP, Gottschalk P, Hirano T, Iwata H, Jurasinski G, Kang M, Koebsch F, Mammarella I, Nilsson MB, Ono K, Peichl M, Peltola O, Ryu Y, Sachs T, Sakabe A, Sparks JP, Tuittila E, Vourlitis GL, Wong GX, Windham-Myers L, Poulter B, Jackson RB. 2021. Identifying dominant environmental predictors of freshwater wetland methane fluxes across diurnal to seasonal time scales. *Glob Change Biol* 27:3582–3604.
- Koebsch F, Jurasinski G, Koch M, Hofmann J, Glatzel S. 2015. Controls for multi-scale temporal variation in ecosystem methane exchange during the growing season of a permanently inundated fen. *Agricultural and Forest Meteorology* 204:94–105.
- Korrensalo A, Alekseychik P, Hájek T, Rinne J, Vesala T, Mehtätalo L, Mammarella I, Tuittila E-S. 2017. Species-specific temporal variation in photosynthesis as a moderator of peatland carbon sequestration. *Biogeosciences* 14:257–269.
- Kostka JE, Weston DJ, Glass JB, Lilleskov EA, Shaw AJ, Turetsky MR. 2016. The Sphagnum microbiome: new insights from an ancient plant lineage. *New Phytol* 211:57–64.
- Kox MAR, van den Elzen E, Lamers LPM, Jetten MSM, van Kessel MAHJ. 2020. Microbial nitrogen fixation and methane oxidation are strongly enhanced by light in Sphagnum mosses. *AMB Expr* 10:61.
- Lai DYF. 2009. Methane Dynamics in Northern Peatlands: A Review. *Pedosphere* 19:409–421.
- Leroy F, Gogo S, Guimbaud C, Bernard-Jannin L, Hu Z, Laggoun-Défarge F. 2017. Vegetation composition controls temperature sensitivity of CO₂ and CH₄ emissions and DOC concentration in peatlands. *Soil Biology and Biochemistry* 107:164–167.
- Lhosmot A, Steinmann M, Binet P, Gandois L, Moquet J-S, Stefani V, Toussaint M-L, Boetsch A, Loup C, Essert V, Bertrand G. in review. Origin and fate of dissolved inorganic carbon in a karst groundwater fed peatland using $\delta^{13}\text{C}_{\text{DIC}}$. *Chemical Geology*.
- Lhosmot A, Collin L, Magnon G, Steinmann M, Bertrand C, Stefani V, Toussaint M, Bertrand G. 2021. Restoration and meteorological variability highlight nested water supplies in middle altitude/latitude peatlands: Towards a hydrological conceptual model of the Frasne peatland, Jura Mountains, France. *Ecohydrology* 14. <https://onlinelibrary.wiley.com/doi/https://doi.org/10.1002/eco.2315>. Last accessed 04/06/2021
- Li Q, Gogo S, Leroy F, Guimbaud C, Laggoun-Défarge F. 2021. Response of Peatland CO₂ and CH₄ Fluxes to Experimental Warming and the Carbon Balance. *Front Earth Sci* 9:631368.
- Loisel J, Gallego-Sala AV, Amesbury MJ, Magnan G, Anshari G, Beilman DW, Benavides JC, Blewett J, Camill P, Charman DJ, Chawchai S, Hedgpeth A, Kleinen T, Korhola A, Large D, Mansilla CA, Müller J, van Bellen S, West JB, Yu Z, Bubier JL, Garneau M, Moore T, Sannel ABK, Page S, Väiliranta M, Bechtold M, Brovkin V, Cole LES, Chanton JP, Christensen TR, Davies MA, De Vleeschouwer F, Finkelstein SA, Frolking S, Gałka M, Gandois L, Girkin N, Harris LI, Heinemeyer A, Hoyt AM, Jones MC, Joos F, Juutinen S, Kaiser K, Lacourse T, Lamentowicz M, Larmola T, Leifeld J, Lohila A, Milner AM, Minkkinen K, Moss P, Naafs BDA, Nichols J, O'Donnell J, Payne R, Philben M, Piilo S, Quillet A, Ratnayake AS, Roland TP, Sjögersten S, Sonnentag O, Swindles GT, Swinnen W, Talbot J, Treat C, Valach AC, Wu J. 2021. Expert assessment of future vulnerability of the global peatland carbon sink. *Nat Clim Chang* 11:70–77.
- Long KD, Flanagan LB, Cai T. 2009. Diurnal and seasonal variation in methane emissions in a northern Canadian peatland measured by eddy covariance. *Global Change Biology* 16:2420–2435.
- Mauder M, Cuntz M, Drüe C, Graf A, Rebmann C, Schmid HP, Schmidt M, Steinbrecher R. 2013. A strategy for quality and uncertainty assessment of long-term eddy-covariance measurements. *Agricultural and Forest Meteorology* 169:122–135.
- Mauder M, Foken T. 2011. Documentation and Instruction Manual of the Eddy-Covariance Software Package TK3 (Project report, research report, survey).
- McKenzie JM, Siegel DI, Rosenberry DO, Glaser PH, Voss CI. 2007. Heat transport in the Red Lake Bog, Glacial Lake Agassiz Peatlands. *Hydrol Process* 21:369–378.
- Mikkilä C, Sundh I, Svensson BH, Nilsson M. 1995. Diurnal Variation in Methane Emission in Relation to the Water Table, Soil Temperature, Climate and Vegetation Cover in a Swedish Acid Mire. *Biogeochemistry* 28:93–114.
- Mitra B, Minick K, Miao G, Domec J-C, Prajapati P, McNulty SG, Sun G, King JS, Noormets A. 2020. Spectral evidence for substrate availability rather than environmental control of methane emissions from a coastal forested wetland. *Agricultural and Forest Meteorology* 291:108062.
- Moore TR, Lafleur PM, Poon DMI, Heumann BW, Seaquist JW, Roulet NT. 2006. Spring photosynthesis in a cool temperate bog. *Global Change Biology* 12:2323–2335.
- Morin TH. 2019. Advances in the Eddy Covariance Approach to CH₄ Monitoring Over Two and a Half Decades. *J Geophys Res Biogeosci* 124:453–460.
- Murray KJ, Tenhunen JD, Nowak RS. 1993. Photoinhibition as a control on photosynthesis and production of Sphagnum mosses. *Oecologia* 96:200–207.
- Nadeau DF, Rousseau AN, Coursolle C, Margolis HA, Parlange MB. 2013. Summer methane fluxes from a boreal bog in

- northern Quebec, Canada, using eddy covariance measurements. *Atmospheric Environment* 41:464–474.
- Nedwell DB, Watson A. 1995. CH₄ production, oxidation and emission in a U.K. ombrotrophic peat bog: Influence of SO₂— from acid rain. *Soil Biology and Biochemistry* 27:893–903.
- Norby RJ, Childs J, Hanson PJ, Warren JM. 2019. Rapid loss of an ecosystem engineer: Sphagnum decline in an experimentally warmed bog. *Ecol Evol* 9:12571–12585.
- Papale D, Reichstein M, Aubinet M, Canfora E, Bernhofer C, Kutsch W, Longdoz B, Rambal S, Valentini R, Vesala T, Yakir D. 2006. Towards a standardized processing of Net Ecosystem Exchange measured with eddy covariance technique: algorithms and uncertainty estimation. *Biogeosciences* 3:571–583.
- Parmentier FJW, van Huissteden J, Kip N, Op den Camp HJM, Jetten MSM, Maximov TC, Dolman AJ. 2011. The role of endophytic methane-oxidizing bacteria in submerged Sphagnum in determining methane emissions of Northeastern Siberian tundra. *Biogeosciences* 8:1267–1278.
- Raghoebarsing AA, Smolders AJP, Schmid MC, Rijpstra WIC, Wolters-Arts M, Derksen J, Jetten MSM, Schouten S, Sininghe Damsté JS, Lamers LPM, Roelofs JGM, Op den Camp HJM, Strous M. 2005. Methanotrophic symbionts provide carbon for photosynthesis in peat bogs. *Nature* 436:1153–1156.
- Rey-Sanchez C, Bohrer G, Slater J, Li Y-F, Grau-Andrés R, Hao Y, Rich VI, Davies GM. 2019. The ratio of methanogens to methanotrophs and water-level dynamics drive methane transfer velocity in a temperate kettle-hole peat bog. *Biogeosciences* 16:3207–3231.
- Riutta T, Korrensalo A, Laine AM, Laine J, Tuittila E-S. 2020. Interacting effects of vegetation components and water level on methane dynamics in a boreal fen. *Biogeosciences* 17:727–740.
- Rosset T, Gandois L, Le Roux G, Teisserenc R, Durantez Jimenez P, Camboulive T, Binet S. 2019. Peatland Contribution to Stream Organic Carbon Exports From a Montane Watershed. *J Geophys Res Biogeosci* 124:3448–3464.
- Rovira AD. 1969. Plant Root Exudates. *Botanical Review* 35:35–57.
- Rubel F, Brugger K, Haslinger K, Auer I. 2017. The climate of the European Alps: Shift of very high resolution Köppen-Geiger climate zones 1800–2100. *metz* 26:115–25.
- Salmon E, Jégou F, Guenet B, Jourdain L, Qiu C, Bastrikov V, Guimbaud C, Zhu D, Ciais P, Peylin P, Gogo S, Laggoun-Défarge F, Aurela M, Bret-Harte MS, Chen J, Chojnicki BH, Chu H, Edgar CW, Euskirchen ES, Flanagan LB, Fortuniak K, Holl D, Klatt J, Kolle O, Kowalska N, Kutzbach L, Lohila A, Merbold L, Pawlak W, Sachs T, Ziemlińska K. 2021. Assessing methane emissions for northern peatlands in ORCHIDEE-PEAT revision 7020. *Biogeosciences* [online] <https://gmd.copernicus.org/preprints/gmd-2021-280/>. Last accessed 06/01/2022
- Saunio M, Stavert AR, Poulter B, Bousquet P, Canadell JG, Jackson RB, Raymond PA, Dlugokencky EJ, Houweling S, Patra PK, Ciais P, Arora VK, Bastviken D, Bergamaschi P, Blake DR, Brailsford G, Bruhwiler L, Carlson KM, Carrol M, Castaldi S, Chandra N, Crevoisier C, Crill PM, Covey K, Curry CL, Etiope G, Frankenberg C, Gedney N, Hegglin MI, Höglund-Isaksson L, Hugelius G, Ishizawa M, Ito A, Janssens-Maenhout G, Jensen KM, Joos F, Kleinen T, Krummel PB, Langenfelds RL, Laruelle GG, Liu L, Machida T, Maksyutov S, McDonald KC, McNorton J, Miller PA, Melton JR, Morino I, Müller J, Murguía-Flores F, Naik V, Niwa Y, Noce S, O'Doherty S, Parker RJ, Peng C, Peng S, Peters GP, Prigent C, Prinn R, Ramonet M, Regnier P, Riley WJ, Rosentretter JA, Segers A, Simpson IJ, Shi H, Smith SJ, Steele LP, Thornton BF, Tian H, Tohjima Y, Tubiello FN, Tsuruta A, Viovy N, Voulgarakis A, Weber TS, van Weele M, van der Werf GR, Weiss RF, Worthy D, Wunch D, Yin Y, Yoshida Y, Zhang W, Zhang Z, Zhao Y, Zheng B, Zhu Q, Zhu Q, Zhuang Q. 2020. The Global Methane Budget 2000–2017. *Earth Syst Sci Data* 12:1561–1623.
- Sebacher DI, Harriss RC, Bartlett KB. 1985. Methane Emissions to the Atmosphere Through Aquatic Plants. *J Environ Qual* 14:40–46.
- Shannon RD, White JR, Lawson JE, Gilmour BS. 1996. Methane Efflux from Emergent Vegetation in Peatlands. *The Journal of Ecology* 84:239.
- Shi Y, Wang Z, He C, Zhang X, Sheng L, Ren X. 2017. Using ¹³C isotopes to explore denitrification-dependent anaerobic methane oxidation in a paddy-peatland. *Sci Rep* 7:40848.
- Smemo KA, Yavitt JB. 2011. Anaerobic oxidation of methane: an underappreciated aspect of methane cycling in peatland ecosystems? *Biogeosciences* 8:779–793.
- Song L, Gilbert D, Wu D. 2016. Vertical micro-distribution of microbial communities living in Sphagnum fallax. *Aquat Microb Ecol* 77:1–10.
- Stepniewska Z, Goraj W. 2014. Transformation of methane in peatland environments. *Forest Research Papers* 75:101–110.
- Ström L, Ekberg A, Mastepanov M, Røjle Christensen T. 2003. The effect of vascular plants on carbon turnover and methane emissions from a tundra wetland. *Global Change Biology* 9:1185–1192.
- Sundh I, Mikkilä C, Nilsson M, Svensson BH. 1995. Potential aerobic methane oxidation in a Sphagnum-dominated peatland—Controlling factors and relation to methane emission. *Soil Biology and Biochemistry* 27:829–837.
- Turetsky MR, Treat CC, Waldrop MP, Waddington JM, Harden JW, McGuire AD. 2008. Short-term response of methane fluxes and methanogen activity to water table and soil warming manipulations in an Alaskan peatland. *J Geophys Res* 113:1–15.
- Turetsky MR, Kotowska A, Bubier J, Dise NB, Crill P, Hornbrook ERC, Minkinen K, Moore TR, Myers-Smith IH, Nykänen H, Olefeldt D, Rinne J, Saarnio S, Shurpali N, Tuittila E-S, Waddington JM, White JR, Wickland KP, Wilkening M. 2014. A synthesis of methane emissions from 71 northern, temperate, and subtropical wetlands. *Glob Change Biol* 20:2183–2197.
- Ueyama M, Yazaki T, Hirano T, Futakuchi Y, Okamura M. 2020. Environmental controls on methane fluxes in a cool temperate bog. *Agricultural and Forest Meteorology* 281:107852.
- Vitale D, Fratini G, Bilancia M, Nicolini G, Sabbatini S, Papale D. 2020. A robust data cleaning procedure for eddy covariance flux measurements. *Biogeosciences* 17:1367–1391.
- Vitale D, Papale D, ICOS-ETC Team. 2021. An R Package for Processing and Cleaning Eddy Covariance Flux Measurements. Viterbo, Italy: ICOS-ETC <https://github.com/icos-etc/RFlux>
- van Winden JF, Reichart G-J, McNamara NP, Benthien A, Damsté JSSinninghe. 2012. Temperature-Induced Increase in Methane Release from Peat Bogs: A Mesocosm Experiment. Treseder K, editor. *PLoS ONE* 7:e39614.

- Waddington JM, Roulet NT, Swanson RV. 1996. Water table control of CH₄ emission enhancement by vascular plants in boreal peatlands. *J Geophys Res* 101:22775–22785.
- Waldo NB, Hunt BK, Fadely EC, Moran JJ, Neumann RB. 2019. Plant root exudates increase methane emissions through direct and indirect pathways. *Biogeochemistry* 145:213–234.
- Whiting GJ, Chanton JP, Bartlett DS, Happell JD. 1991. Relationships between CH₄ emission, biomass, and CO₂ exchange in a subtropical grassland. *J Geophys Res* 96:13067.
- Wilczak JM, Oncley SP, Stage SA. 2001. Sonic Anemometer Tilt Correction Algorithms. *Boundary-Layer Meteorology* 99:127–150.
- Windsor J, Moore TR, Roulet NT. 1992. Episodic fluxes of methane from subarctic fens. *Can J Soil Sci* 72:441–452.
- Wutzler T, Lucas-Moffat A, Migliavacca M, Knauer J, Sickel K, Šigut L, Menzer O, Reichstein M. 2018. Basic and extensible post-processing of eddy covariance flux data with REddyProc. *Biogeosciences* 15:5015–5030.
- Xu J, Morris PJ, Liu J, Holden J. 2018. PEATMAP: Refining estimates of global peatland distribution based on a meta-analysis. *CATENA* 160:134–140.
- Yavitt JB, Lang GE, Sexstone AJ. 1990. Methane fluxes in wetland and forest soils, beaver ponds, and low-order streams of a temperate forest ecosystem. *J Geophys Res* 95:22463.
- Zhang H, Tuittila E, Korrensalo A, Laine AM, Uljas S, Welti N, Kerttula J, Maljanen M, Elliott D, Vesala T, Lohila A. 2021. Methane production and oxidation potentials along a fen-bog gradient from southern boreal to subarctic peatlands in Finland. *Glob Change Biol* 27:4449–4464.

Springer Nature or its licensor (e.g. a society or other partner) holds exclusive rights to this article under a publishing agreement with the author(s) or other rightsholder(s); author self-archiving of the accepted manuscript version of this article is solely governed by the terms of such publishing agreement and applicable law.